Experimental Evaluation of the Performance of 3D Printed Composite Auxetic Structure under Compressive Loads

Mao Yanjun

American Community School of Abu Dhabi, Unnamed Road, Saddiyat Island, Abu Dhbai, United Arab Emirates
51140@acs.sch.ae

Abstract: Due to the deforming nature of their designs, most auxetic structures inherently lack stiffness. As a result, they are often unsuitable for applications requiring both high stiffness and energy absorption. Previous studies in this area have typically focused on a limited number of configurations without systematic, cross-study comparisons. This research aims to address this gap by improving upon several high-performing auxetic designs from prior literature and conducting a standardized comparative analysis. Four enhanced designs, based on promising configurations from previous studies, were 3D printed using PLA-CF filaments. Their compressive properties were then evaluated using a universal testing machine. The resulting data was processed to determine each design's stress-strain curve, total energy absorbed, and specific energy absorption (SEA). The results indicate that the improved design based on the work of Tabacu et al. performed the best, exhibiting the highest peak stress and superior energy absorption. The analysis reveals that designs with support structures acting either parallel or perpendicular to the loading axis perform more poorly than designs that distribute the load more evenly. The value of this research lies in its standardized cross-comparison of different auxetic structures from different studies, all tested with the same material and parameters. This provides a clear benchmark for performance. Additionally, by enhancing existing designs based on methods proposed in other research, this study further explores and validates the potential of these advanced auxetic configurations.

1. Introduction

Auxetic structures are defined as structures that display a negative Poisson's ratio when under load. This characteristic allows the structure to collapse inward laterally when experiencing a compressive longitudinal force, thus enabling the overall structure to maintain cohesion after absorbing the energy from the load. The impact-resistant, fracture-resistant, and indentation-resistant properties of auxetic structures give them the potential to be applied to applications such as highway crash barriers, anti-blast barriers, and other impact-resistant or energy-absorbing

applications [1,2,3].

3D printing is a manufacturing method capable of fabricating the complex geometries required for various auxetic structures within a relatively short prototyping cycle. Furthermore, 3D printing enables the use of composite filaments to produce structures that are both lightweight and high-strength, making them suitable for demanding industrial applications. Therefore, this paper investigates the performance of 3D-printed composite auxetic structures under compressive loads.

However, due to their inherent deforming nature, most auxetic structures lack stiffness[4]. As a result, their application is limited in scenarios requiring both high stiffness and energy absorption. While previous research has explored various possible structural configurations that are topologically optimized to determine which configuration offers the best energy absorption and strain performance, these studies were often limited in scope. Typically, they focused on only two to four configurations without cross-referencing another research. This study aims to build upon these previous findings by systematically improving and comparing several high-performing configurations from different studies.

This research will first review various optimized auxetic structures that have performed well in previous studies. Then, based on the existing literature, structural alterations will be introduced to optimize both energy absorption and stiffness. Four distinct designs will then be 3D printed using a carbon composite filament and tested under compressive loading. The primary aim of this research is to identify the optimal auxetic structure design, fabricated from carbon composite materials, that exhibits superior compressive performance.

2. Materials and Methods

2.1. Material and Equipment

All structures used in this experiment were printed using a Bambu Lab A1 with short-fiber carbon composite filaments. Short-fiber carbon composite filaments were chosen due to their high compressive performance, which is enabled by the chopped carbon fibers within the filament. This particular filament, made by Bambu Lab, consists of short carbon fibers suspended in PLA plastic and is therefore abbreviated as PLA-CF. Compared to continuous-fiber filaments, short-fiber filaments allow for the fabrication of more complex geometries and a more practical printing process, while still providing significantly higher stiffness than pure polymer filaments.

The four different auxetic specimens were then tested for their compressive performance using a universal testing machine. The specimens were uniaxially compressed at a loading velocity of 2 mm/min. This slow speed was chosen so that each stage of the specimen's failure could be observed and recorded in high detail.

The compressive performance of the ASL samples was tested using a WDW-100M universal testing machine (UTM), manufactured by Jinan Chenda. This machine has a maximum force capacity of 100 kN, which was sufficient to fully compress the samples. The remaining designs, which had lower anticipated failure forces, were compressed using a smaller UTM with a 5 kN capacity.

2.2. Shape optimization

A traditional unaltered auxetic structure that is unaltered as shown in Figure 1. is used as the control specimen.

According to research by Gohar et al., an effective method for increasing the compressive performance of an auxetic structure is to strategically add material at locations of high stress concentration [4]. In this study, this principle was applied to high-performing designs from previous

literature to further enhance their performance (see Figure 2). Additionally, research by Zhang et al. suggests that incorporating internal support structures can increase a design's post-failure stiffness, thereby increasing its overall energy absorption [5]. This concept was used to further improve the high-performing "mixed star" structure from Gohar et al. (see Figure 3).
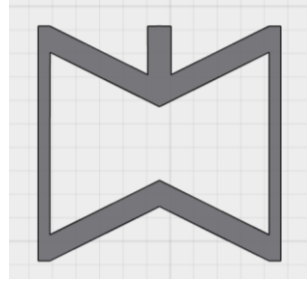

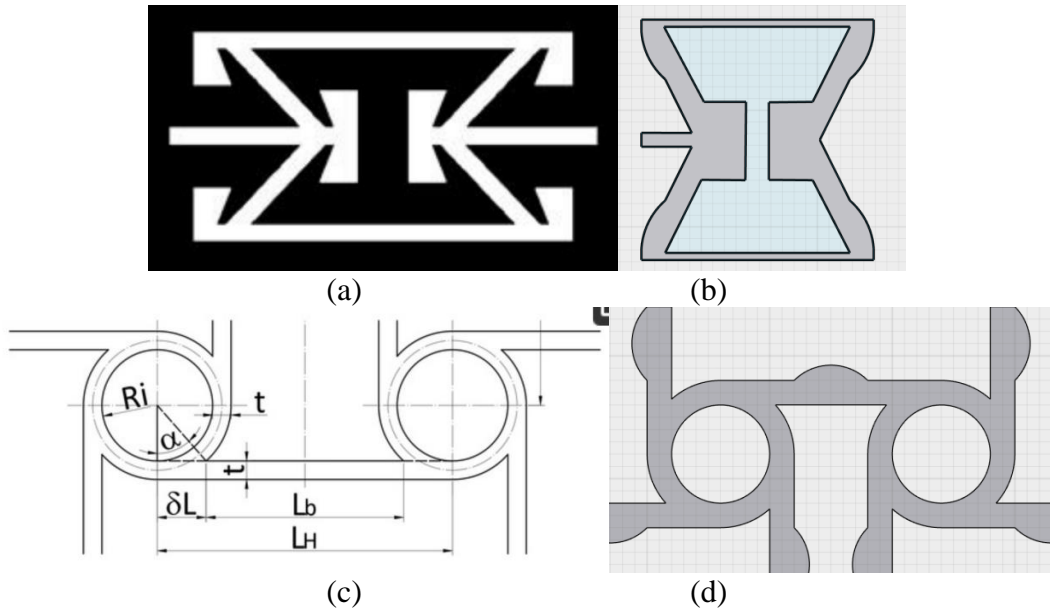
Figure 1 Traditional Auxetic Structure (TAS)

(a)   (b)

(c)   (d)

Figure 2(a) Original design from Zhang et.al[5] (b) Optimized Design by increasing material lat stress locations/ Auxetic Structure with Internal Support (ASIS) (c) Original design from Tabacu et.al[6] (d) Optimized Design by increasing material at stress locations/Auxetic structure with Ligaments (ASL)

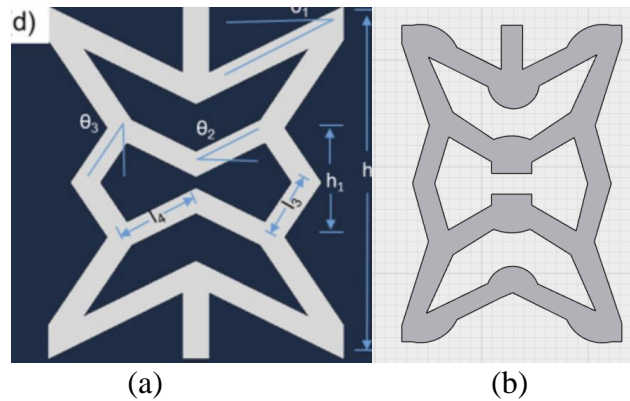(a)   (b)

Figure 3 (a) Original Design from Gohar et.al (b) Optimized Design by increasing material at stress locations and enlarging internal support structures/Mixed Star Structure (MSS)

2.3. Fabrication of specimens

The four auxetic structures were designed using Shapr3D and subsequently exported as .step files. These files were then imported into Bambu Studio software and sliced to prepare them for printing. The experiment utilized a Bambu Lab A1 printer. This model was chosen for its high printing speed and PLA-CF compatibility, which was ideal for the large number of samples required for this study. A 0.6 mm nozzle was used to maintain a high print speed, and the printing temperature was set to 220 ℃. After printing, all parts were annealed on the print bed at 60 ℃ for 8 hours to ensure optimal layer cohesion. The "Arachne" wall generation algorithm was used to minimize printing defects in thin-walled sections. Each design was printed three times to account for and reduce errors arising from manufacturing inconsistencies. Table 1 shows the measured parameters of the initial state for four printed specimens with different structures.

Table 1 Specimen Dimensions

Name	Width (mm)	Height (mm)	Depth (mm)
TAS	52.5	37.2	20
ASIS	54.4	37.6	20
ASL	57.0	39.0	20
MSS	50.7	38.15	20

2.4. Experiment Procedures

The experiment procedure is as follows; first the specimen is placed on to the compression plate of the Universal testing machine. The manual control device can be used to lower the top plate until the top plate is just in contact with the specimen. The loading process can begin with the load speed set to 2mm/min and all values initialized. The criteria for determining when the loading can be terminated is when the latest values have exceeded the previous highest values and does not have a downwards trend, and the specimen appears to have been fully compressed. Each auexteic structure design has been printed 3 times using the identical printing parameters, therefor each design is tested 3 times to reduce error.

3. Experiment results

Table 2 Dimensional comparison of pre-post compression specimens

Specimen Code	Initial Width(mm)	Initial Height(mm)	Initial Depth(mm)	Final Width (mm)	Final Height(mm)	Final Depth(mm)
TAS_1	52.5	37.2	20.0	53.00	20.67	20.28
ASIS_1	54.4	37.6	20.0	59.00	23.74	20.34
ASL_1	57.0	39.0	20.0	58.76	19.16	20.40
MSS_1	50.7	38.15	20.0	52.91	26.80	20.35
TAS_2	52.5	37.2	20.0	53.27	20.09	20.33
ASIS_2	54.4	37.6	20.0	58.09	24.62	20.27
ASL_2	57.0	39.0	20.0	55.68	19.82	20.90
MSS_2	50.7	38.15	20.0	55.13	26.40	20.49
TAS_3	52.5	37.2	20.0	54.05	18.98	20.33
ASIS_3	54.4	37.6	20.0	60.10	22.59	20.38
ASL_3	57.0	39.0	20.0	56.77	19.88	20.96
MSS_3	50.7	38.15	20.0	54.32	25.96	20.43

Table 2 shows the dimensional comparison analysis of specimens before and after compression testing. The dimensional comparison of specimens before and after compression testing reveals critical insights into the material's deformation behavior, structural integrity, and stability under

compressive loads.

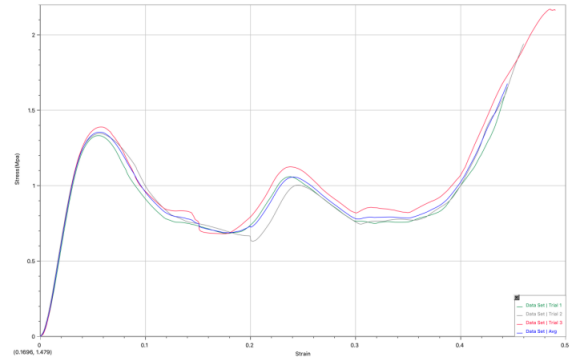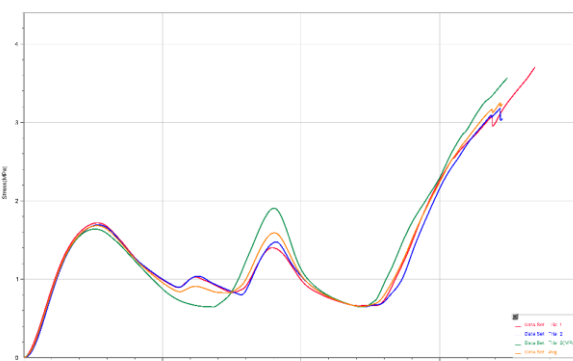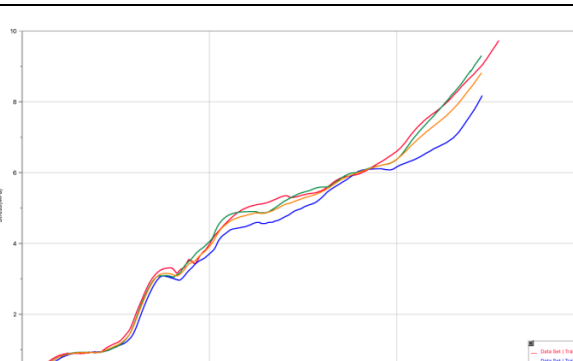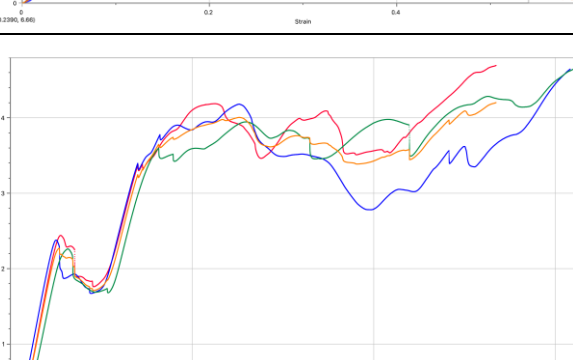Table 3 Stress-Strain Curve of each trial and average

TSA	
ASIS	
ASL	
MSS	

Table 3 presents the stress-strain curves for each trial along with the average curves. As can be

observed, the ASL structure exhibits the smoothest curve, whereas the curves of the other three structures all demonstrate points of stress concentration.

The data in Table 3 indicate that the ASL structure achieved the highest peak stress, exceeding 8 MPa. This superior performance can be attributed to its design, which effectively converts axial compressive displacement into the rotational motion of its internal circular elements and transfers the stress evenly throughout the structure. This mechanism distributes the load through both the tension and compression of each ligament, allowing for uniform densification and simultaneous compression across the entire structure. This is in sharp contrast to the other three designs, in which failure occurs progressively, layer by layer. In those cases, stress is concentrated on a single layer at any given moment rather than being distributed across the entire structure. This finding suggests that the concept of using vertical support structures to resist deformation is less effective than ASL's ligament-based design, as vertical supports tend to bend or buckle under sufficient load, which causes an uneven stress distribution.

Figures 4-7 shows the stress-strain graph comparison with qualitative deformation profiles for each structure.
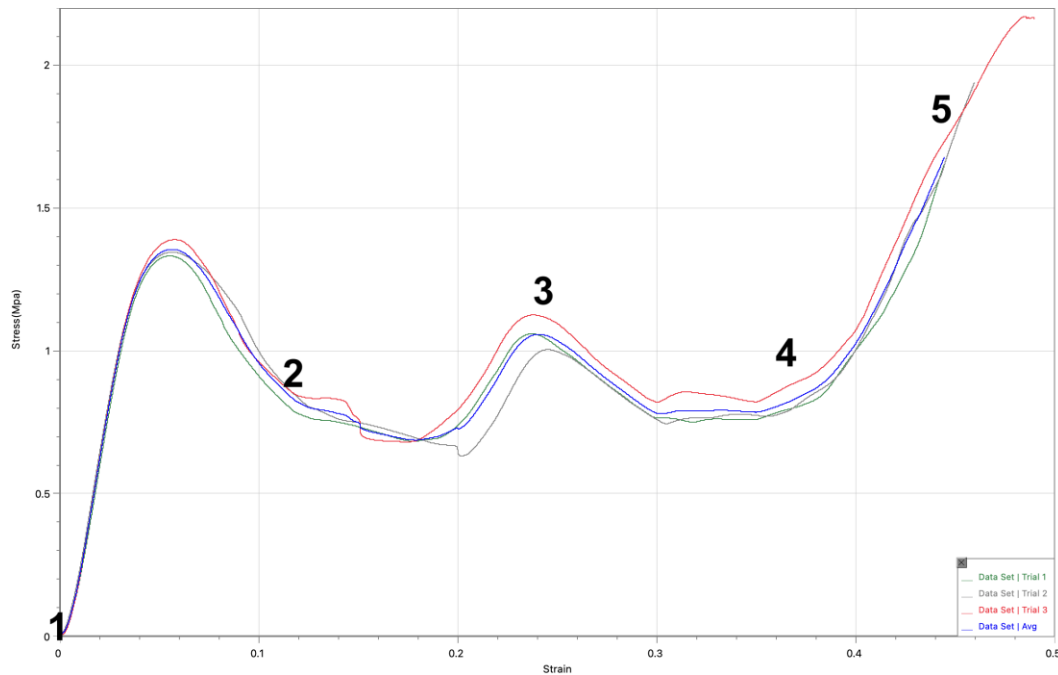

Figure 4 Stress-Strain profile of TAS

At Stage 1, all vertical struts remained undeformed and provided a reaction force that was intact until the first yield point (between points 1 and 2). Subsequently, after the penultimate layer had fully failed and the bottommost layer had partially failed, the top two layers still had not started to deform. This provided the necessary strength until the second yield point at point 3. After this point, all vertical structures had deformed, and the whole structure entered its plastic deformation zone at point 4. This process continued until the structure was fully compressed in Stage 5.(figure 4)
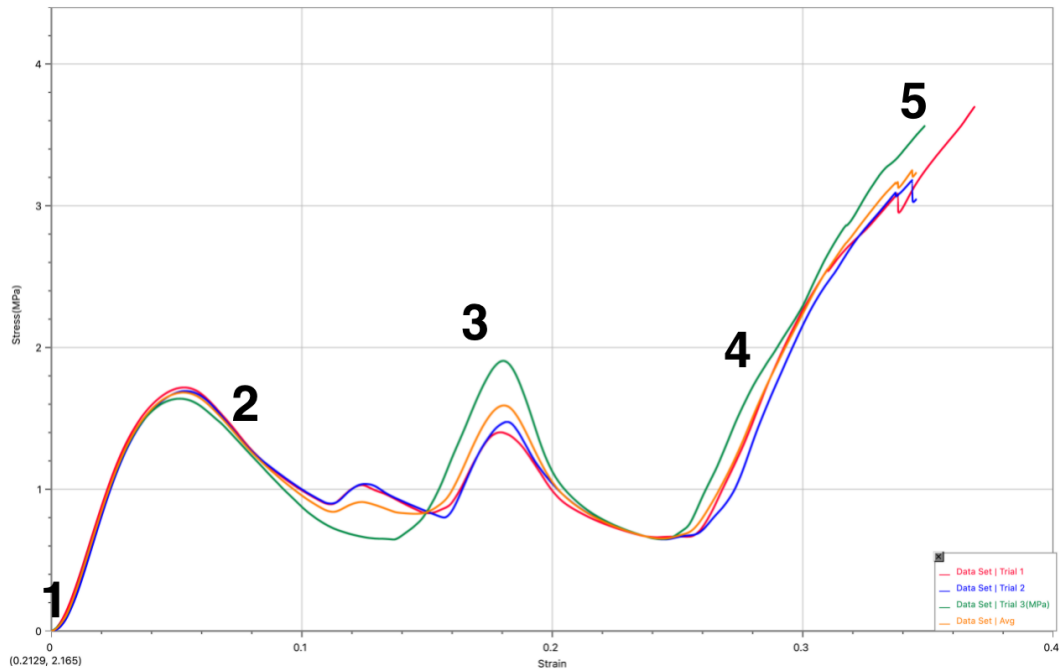
Figure 5 Stress-Strain profile of ASIS

In Stage 1, all vertical struts remained undeformed and provided a reaction force that was intact until the first yield point (between points 1 and 2). The first yield point was marked by the plastic deformation of the middlemost layer. After the middle section had fully collapsed, the vertical internal support structures in all layers were compressed and made contact with each other. This contact provided the necessary strength until the second yield point. After this point, the support structures started to slide past each other due to the torque generated by the yielding of the solid vertical elements. Once the two middle layers were fully compressed, the internal support structure in the bottommost layer provided resistance until the third and final yield point. (Figure 5)
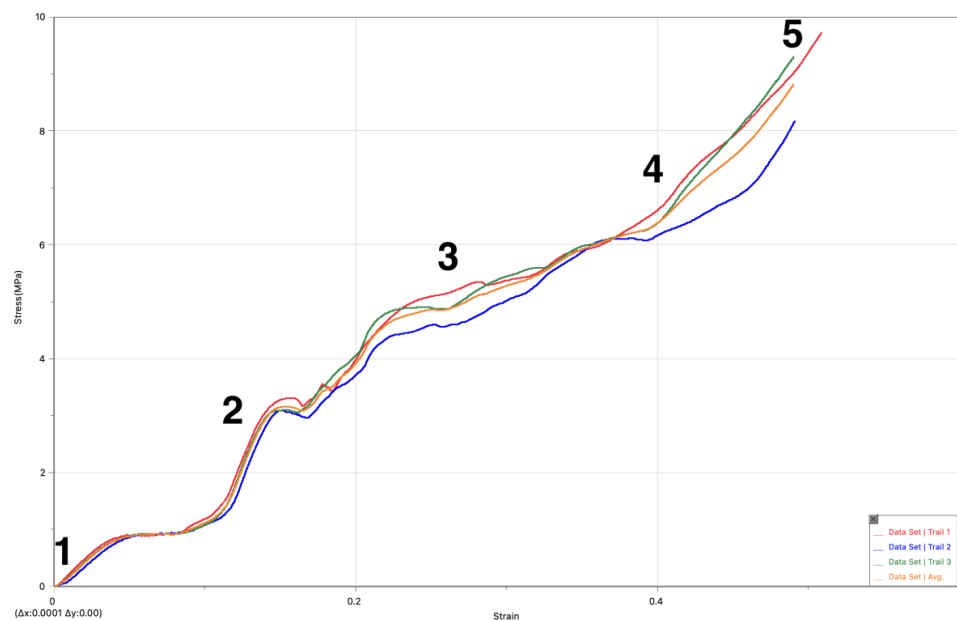

Figure 6 Stress-Strain profile of ASL

In Stage 1, all structures were intact, and the ligaments were not under tension. After compression began, the torque generated by the outermost ligaments caused the circular structures to deform plastically and bend outward. This phenomenon was observed in the plastic deformation zone between points 1 and 2. This bending caused the gaps between the ligaments to close until all parallel ligaments made contact, as seen in Stage 2. This contact gave the structure renewed strength until the second yield point. The second yield point was marked by audible cracking sounds from ligaments fracturing under both tension and compression, which caused a small dip in stress. From this point onward, the circular structures in all layers began to deform uniformly, creating a roughly linear stress-strain response until they were fully compressed. (Figure 6)
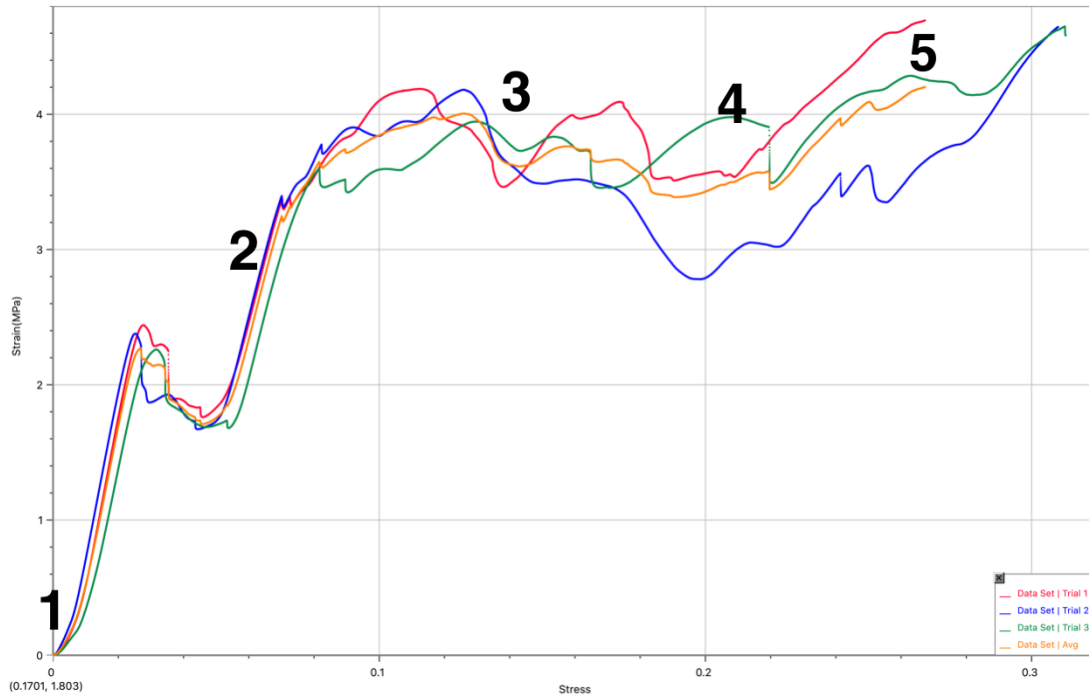

Figure 7 Stress-Strain profile of ASL

In Stage 1, all vertical struts remained undeformed and provided a reaction force that was intact until the first yield point (between points 1 and 2). The first yield point was marked by audible cracking sounds, indicating the fracture of the horizontal support structures. This event correlates with the sharp drop in stress observed after this point. This initial failure was followed by a short period of plastic deformation, during which the two internal struts of each cell began to bend and eventually contact each other. This contact provided renewed strength to the structure until the second yield point (between Stages 2 and 3). After this, the two struts in each cell started to slide past each other, generating a torque that allowed the structure to deform plastically. This process continued from Stage 3 to Stage 5, at which point the structure was fully compressed. (Figure 7)

Equation (1) for Total Energy Absorption :

$$W = \int_0^{\Delta l \leq 14} F(\Delta l) \, dF \tag{1}$$

Where W = Total Energy Absorbed; Δl = Change of Specimen Length; F = Force

Table 4 Total Energy Absorption

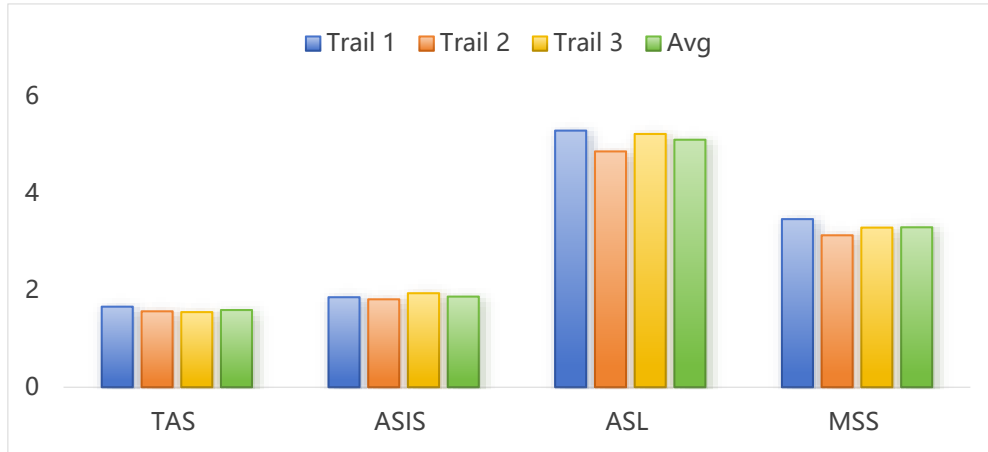| Total Energy Absorption (Δl ≤ 14mm) (J x 10^4)	TAS	ASIS	ASL	MSS
Trial 1	1.664	1.860	5.301	3.473
Trial 2	1.567	1.815	4.869	3.138
Trial 3	1.551	1.943	5.229	3.298
Avg	1.594	1.873	5.113	3.303

Figure 8 Total Energy Absorbed

Equation (2) for Specific Energy Absorption:

$$W_s = W = \int_0^{\Delta l \leq 14} F(\Delta l) \, dF \, /m \qquad (2)$$

Where W_s= Specific Energy Absorption; m= Total Mass of Specimen

Table 5: Specific Energy Absorption

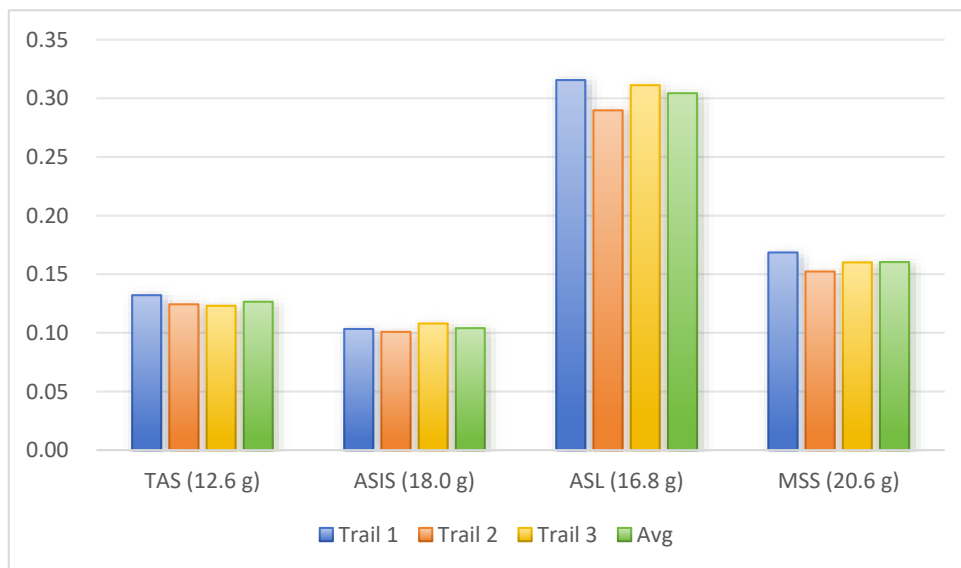| Specific Energy Absorption (J x 10^4 /g)	TAS (12.6 g)	ASIS (18.0 g)	ASL (16.8 g)	MSS (20.6 g)
Trial 1	0.13206	0.10333	0.31554	0.16859
Trial 2	0.12437	0.10083	0.28982	0.15233
Trial 3	0.12310	0.10794	0.31125	0.16010
Avg	0.12651	0.10406	0.30435	0.16034

Figure 9 Specific Energy Absorption

As can be seen from Figures 8 and 9, the total energy absorption and specific energy absorption of the four different structures exhibit identical trends, thereby validating the feasibility of the experimental approach.

As can be seen from table 4, ASL has the highest total energy absorbed at an average of 1.415 J and as can be seen from table 5,it also has the highest specific energy absorption at an average of 0.30435E4/g. So ASL has the best overall compressive performance.

4. Conclusion

This paper investigated the compressive performance of auxetic structures fabricated using FDM 3D printing and PLA-CF filaments. The testing involved compressing the auxetic structures to evaluate the stress-strain profile and energy absorption capabilities of each design. The results show that the ASL structure, which was based on a design by Tabacu et al. and improved using methods suggested by Gohar et al., performed the best overall. The ASL structure exhibited the highest peak stress before full compression; it also had the highest total and specific energy absorption. This proves the advantage of circular-ligament-based designs over those that rely on support structures acting parallel or perpendicular to the axis of loading. This research could be further improved by compressing each structure along both the y-axis and the x-axis, which would allow the optimal orientation for each design to be more accurately determined.

The value of this research is that it compared different designs of auxetic structures from different studies and tested them using the same material and parameters, thus providing a clear benchmark of which design performs best. Additionally, the designs were improved based on methods proposed in other research, further exploring their potential. Future work on auxetic structures can explore more methods for improving stiffness while simultaneously increasing the energy absorption capacity of different designs. Furthermore, different stress-strain profiles can be explored for use in various applications.

References

[1] Sengul, Mustafa , et al. "Real-World Applications of Auxetic Structures in Engineering: A Review." Structures, vol. 80, no. 80, July 2025.

[2] Bohara, Rajendra Prasad, et al. "Anti-Blast and -Impact Performances of Auxetic Structures: A Review of Structures, Materials, Methods, and Fabrications." Engineering Structures, vol. 276, Feb. 2023, p. 115377, https://doi.org/10.1016/j.engstruct.2022.115377. Accessed 9 Dec. 2022.

[3] Pereira, Felipe, et al. "Development and Applications of 3D Printing-Processed Auxetic Structures for High-Velocity Impact Protection: A Review." Eng, vol. 4, no. 1, 8 Mar. 2023, pp. 903–940, https: //doi. org/10. 3390/eng4010054.

[4] Gohar, Sohail, et al. "Performance of 3D Printed Topologically Optimized Novel Auxetic Structures under Compressive Loading: Experimental and FE Analyses." Journal of Materials Research and Technology, vol. 15, 13 Aug. 2021, pp. 394–408, https://doi.org/10.1016/j.jmrt.2021.07.149. Accessed 1 May 2025.

[5] Zhang, Xiang Yu, et al. "A Novel Auxetic Metamaterial with Enhanced Mechanical Properties and Tunable Auxeticity." Thin-Walled Structures, vol. 174, May 2022, p. 109162, https://doi.org/10.1016/j.tws.2022.109162.

[6] Tabacu, Stefan, et al. "Complex Analysis of an Auxetic Structure under Compressive Loads." Sustainability, vol. 15, no. 8, 18 Apr. 2023, p. 6805, https://doi.org/10.3390/su15086805. Accessed 1 Jan. 2025.